



Nanostructured materials in agriculture: The influence of bismuth ferrite and graphitic carbon nitride on maize growth performances in Samaru, Nigeria

S.M. Yahaya¹, N. Abdu¹, I.A. Aliyu¹ and B. Mukhtar²

¹Department of Soil Science, Faculty of Agriculture/Institute for Agricultural Research, Ahmadu Bello University, P.M.B. 1044, Zaria, Nigeria

²Department of Chemical Engineering, Faculty of Engineering, Ahmadu Bello University, P.M.B. 1044, Zaria, Nigeria

ABSTRACT

This study explores the application of nanostructured materials, specifically metal-free graphitic carbon nitride ($g\text{-C}_3\text{N}_4$), bismuth ferrite (BiFeO_3), magnesium-doped bismuth ferrite ($\text{Bi}_{0.7}\text{Mg}_{0.3}\text{FeO}_3$), and a heterojunction of $g\text{-C}_3\text{N}_4$ and bismuth ferrite ($g\text{-C}_3\text{N}_4/\text{BiFeO}_3$), in influencing maize growth and performances in Samaru, Nigeria. The study involves the synthesis and characterization of these nanostructured materials, confirming their structural integrity and stability for photocatalytic applications. The greenhouse experiment employs a range of treatments, including a control (no fertilization), +P +K inorganic fertilizer, the recommended farmer's fertilizer rate (120:60:60), and varied levels of the synthesized nanostructured materials (1 g, 2 g and 3 g). The experiment was laid out in a completely randomized design, and maize (SAMMAZ 15) was used as test crop. Graphitic carbon nitride consistently exhibits the highest plant height, while the recommended rate and magnesium-doped bismuth ferrite excelled in stem girth. Root dry weight was significantly higher in the recommended rate and bismuth ferrite treatments, emphasizing their positive influence on root development. Similar trends were observed in shoot dry weight, with the recommended rate outperforming other treatments. Moreover, the study highlights the importance of treatment levels, identifying level 2 (2 g) as optimal for improved maize performance, aligning with the recommended rate of traditional fertilizer application. While nanostructured materials showed promising performances compared to the control, their impact on growth is comparable to conventional fertilizers. This research provides valuable insights into the potential of nanostructured materials in promoting maize growth, emphasizing the need for further exploration of their mechanisms and optimal application levels in agricultural practices.

Keywords: Photocatalysts; nanomaterials; nitrogen fixation; maize, growth performance

INTRODUCTION

In the pursuit of sustainable and innovative agricultural practices, the integration of nanotechnology has emerged as a promising avenue (Dimkpa & Bindraban, 2017; Zhang *et al.*, 2020). As the global demand for food production continues to rise, optimizing agricultural practices becomes imperative. The potential of nanotechnology to revolutionize crop management and improve yield efficiency is a subject of increasing interest. Amidst the challenges posed by climate change, soil degradation, and the quest for eco-friendly agricultural practices, the integration of nanostructured materials stands out as a cutting-edge approach (Babu *et al.*, 2022). Bismuth ferrite and graphitic carbon nitride, the focal points of this study, bring forth the promise of precision agriculture tailored to the needs of Samaru's maize cultivation (Devthade *et al.*, 2018; Hasija *et al.*, 2019; Luo *et al.*, 2022; Mardani, 2017). As the global scientific community continues to unlock the potentials of nanotechnology, this research not only contributes to the broader discourse but also places Samaru, Nigeria, at the forefront of this agricultural revolution. By strategically inserting advanced nanomaterials into the agricultural landscape, we anticipate uncovering insights that transcend local contexts, offering scalable solutions for sustainable maize production worldwide.

This study delves into the application of advanced nanomaterials to enhance crop growth and yield. The focus on bismuth ferrite and graphitic carbon nitride, two distinct nanostructured materials, is particularly relevant in the unique agricultural landscape of Samaru, Nigeria. The experiment explores their influence on maize growth performances, aiming to unravel the nuanced interactions between these nanostructured materials and the specific needs of maize crops in this geographical context. The study contributes to this discourse by not only synthesizing and characterizing novel nanostructured materials but also rigorously testing their impact on maize growth. The outcomes of this research hold the promise of not only advancing our understanding of nanomaterial-crop interactions but also offering practical insights into how these materials can be applied in the context of Nigerian agriculture, specifically in Samaru. In essence, this study represents a crucial step towards harnessing the benefits of nanotechnology for sustainable and enhanced agricultural productivity in the region.

MATERIALS AND METHODS

Soil Sample Collection and Preparation

The soil samples for the experiment were collected from the research field of Institute for Agricultural Research, Ahmadu Bello University, Zaria (latitude 11°10'32" N, longitude 7°36'51" E with elevation of 710 meters above sea level). The soil is classified under the order Alfisols as Haplustalfs of USDA Soil Taxonomy System (Harpstead, 1973). The environment falls under Northern Guinea Savanna zone of Nigeria which has a unimodal rainfall distribution with an average rainfall and temperature of 1051.7 mm and 27.3 °C respectively (Akintola, 2001). It has an annual average sunshine of about 10.5 hours with mean solar radiation of 6.0 kWh/m²/day (Abam *et al.*, 2014). Soil samples were collected randomly in a hectare of land at a depth of 0–15 cm, bulked to make a composite sample and placed inside polythene bag. The samples were taken to the laboratory, spread, air dried, and stored for the routine analysis and subsequent experimentation.

Photocatalysts Synthesis

In the synthesis of catalysts, several methods were employed to create distinct nanomaterials with specific properties. For the production of metal-free graphitic carbon nitride (g-C₃N₄), a pyrolysis technique was utilized, following established procedures (Jin *et al.*, 2018; Katsumata *et al.*, 2013). Eighty grams of melamine, was thermally treated in an alumina crucible at approximately 550 °C for four hours, resulting in the formation of g-C₃N₄ nanostructured powder after cooling and subsequent crushing.

Bismuth ferrite (BiFeO₃) was synthesized through a modified sol-gel method using the citric acid route, as described by Haruna *et al.* (2020). This method involved dissolving precise amounts of analytical-grade Fe(NO₃)₃·9H₂O and Bi(NO₃)₃·5H₂O in distilled water. The mixture was stirred at 90 °C, and citric acid (4.0 x 10⁻¹M) was gradually added while stirring continued for 40 minutes. Ethylene glycol (10 mL) was introduced as a polymerization and structure-directing agent. The solution's pH was maintained at 8 using sodium dodecyl sulfate (0.35M) and ammonium hydroxide (30 % NH₃). After drying and pre-calcination, a pure-phase bismuth ferrite powder was obtained.

For the synthesis of magnesium-doped bismuth ferrite (Bi_{0.7}Mg_{0.3}FeO₃), a similar modified sol-gel approach was employed. This process entailed dissolving specific quantities of Fe(NO₃)₃·9H₂O and Bi(NO₃)₃·5H₂O, and Mg(NO₃)₂ in distilled water, following a procedure akin to that used for bismuth ferrite. The resulting gel was pre-calcined, leading to the formation of pure-phase magnesium-doped bismuth ferrite powder.

Finally, the heterojunction between graphitic carbon nitride and bismuth ferrite nanomaterials was formed using a co-precipitation method. A measured amount of as-prepared g-C₃N₄ was combined with analytical-grade Bi(NO₃)₃·5H₂O and Fe(NO₃)₃·9H₂O in ethylene glycol, and the mixture underwent a series of stirring, sonification, and heating steps, ultimately yielding the powdered g-C₃N₄/BiFeO₃ (Acharya & Parida, 2020).

Characterization of Synthesized Photocatalysts

The synthesized photocatalysts were methodically characterized through various techniques. Powdered X-ray diffraction (PXRD) analysis was employed to elucidate the crystal structure of the nanostructured materials using a Rigaku Ultima IV X-ray diffractometer with copper (Cu) K α radiation. In this analysis, X-rays are directed at a powdered sample, and the resulting diffraction pattern is recorded on a detector. The diffraction pattern arises from the constructive interference of X-rays scattered by crystal planes within the sample. By analyzing the angles and intensities of these diffraction peaks, the crystal structure, phase composition, and crystallite size of the material can be determined. The data obtained are then compared to known patterns in crystallographic databases to identify the sample's structure.

Fourier transform infrared spectroscopy, performed with a PerkinElmer Spectrum 100n FTIR spectrometer, facilitated the identification of the nanostructured materials' formation, with the resulting spectra analyzed using Origin software. The procedure involves exposing the sample to infrared radiation over a range of frequencies. The molecules in the sample absorb specific infrared wavelengths corresponding to vibrational modes, such as stretching and bending of chemical bonds. The key step is the interferogram acquisition, where the infrared signal is measured as a function of time. This raw data is then transformed into a spectrum using Fourier transformation, revealing absorption peaks at characteristic

frequencies. The resulting FTIR spectrum provides information about the functional groups present in the sample, aiding in molecular identification and structural analysis of organic and inorganic compounds.

Additionally, thermogravimetric analysis carried out in a PerkinElmer Thermal analysis instrument, enabled the assessment of thermal stability and volatile components by monitoring material weight changes during controlled heating. The procedure involves heating the sample in a controlled environment while continuously monitoring its weight. As the temperature increases, the sample undergoes physical and chemical transformations, such as decomposition or volatilization, leading to weight loss. The change in mass is recorded on a thermogravimetric curve. TGA provides insights into material composition, thermal stability, and decomposition kinetics. By analyzing the temperature at which significant mass changes occur, researchers can identify components, determine purity, and assess thermal stability.

Treatments and Experimental Design

The greenhouse experiment included trial with maize (*Zea mays* L.) (SAMMAZ 15) as a test crop. The treatments include control (no fertilization); + P + K (without N); three levels of the recommended NPK fertilizer (120:60:60) at 50%, 100% and 150% ; three levels of graphitic carbon nitride (1 g, 2 g and 3 g); three levels of bismuth ferrite (1 g, 2 g and 3 g); three levels of magnesium doped bismuth ferrite (1 g, 2 g and 3 g); and three levels of heterojunction graphitic carbon nitride/bismuth ferrite (1 g, 2 g and 3 g), replicated three times. The experiment was laid down in completely randomized design.

Planting, Measurements, and Harvesting

Planting was done at two seeds per pot and were later thinned to one plant per pot a week after germination. Plants were irrigated every day as required. Plant growth parameters such as plant height and stem girth were taken two weeks after planting and subsequently after each week until harvest. The plant height was measured using meter rule and stem girth was measured using vernier calliper. Harvesting was done at eight weeks after planting. Thus, plants were carefully removed from the pots, the shoots were cut at the soil surface level using sharp knife. The roots were carefully washed in running tap-water. Both the roots and the shoots were taken to the laboratory and oven dried at 60 °C for two days and the dry weight was measured.

Statistical Data Analysis

The data collected were analyzed using the General Linear Model (GLM) procedure of Analysis of Variance (ANOVA), where a significant difference is observed, post-hoc Tukey honesty significant different test was used for means separation. All analyses were conducted using R-commander (Fox, 2018) in R statistical software (Team, 2017). Graphs were plotted using Origin software (version 9.55).

RESULTS AND DISCUSSION

Characterization of the Synthesized Nanostructured Photocatalysts

Powdered X-ray diffraction (PXRD) analysis revealed characteristic patterns for each material (Figure 1). Graphitic carbon nitride exhibited characteristic peaks at approximately 12° and 28°, attributed to the [100] and [002] planes, aligning with the orthorhombic g-C₃N₄ structure (Thomas *et al.*, 2008) and these matches well with the orthorhombic g-C₃N₄ in the diffraction standard Joint Committee on Powder Diffraction Standards (JCPDS) card no. 87 – 1526 (Wojtyła & Baran, 2021). This represents interfacial stacking and in-plane packing of the graphitic carbon nitride (Hu *et al.*, 2020a). Bismuth ferrite displayed a sharp peak at about 30°, consistent with the [110] facets of pure perovskite-structured BFO according to the powder data JCPDS card no. 73 – 0548 (Azmy *et al.*, 2017). The magnesium-doped bismuth ferrite demonstrated enhanced crystallinity with well-defined peaks, indicating successful incorporation of magnesium ions. The heterojunction of graphitic carbon nitride and bismuth ferrite showed a unique peak at approximately 30°, signifying harmonization between the two catalysts and suggesting potential synergistic effects in photocatalysis.

Fourier transform infrared spectroscopy (FTIR) was used to identify functional groups in the synthesized materials (Figure 2). Graphitic carbon nitride exhibited characteristic bands corresponding to aromatic C = C stretching and = C – H bending vibrations. This proved the formation of graphitic carbon nitride based on the assigned spectra (Chen & Fan, 2017). Furthermore, the sharp band at around 1650 cm⁻¹ can be ascribed to the fine crystallinity of graphitic carbon nitride (Irshad *et al.*, 2022). Bismuth ferrite displayed spectra consistent with its perovskite structure, corroborating the PXRD results. The presence of broad absorbance peak at around 850–1350 cm⁻¹ was assigned to the powdered crystals, signifying the absorption of water molecules onto the surface of the bismuth ferrite (Haruna *et al.*, 2020). Additionally, stretching and bending vibrations at around 600 cm⁻¹ shows the assigned metal–oxygen bonds for Fe–O and O–Fe–O in the perovskite structure (Souza *et al.*, 2010). These confirmed that the materials synthesized have similar structural characteristic and functional groups of the bismuth ferrite perovskite nanomaterials. Magnesium-doped bismuth ferrite and the heterojunction displayed similar functional groups to their parent materials, indicating that doping and heterojunction formation did not significantly alter their chemical compositions.

Thermogravimetric analysis (TGA) was employed to assess the thermal stability of the materials (Figure 3). Graphitic carbon nitride and the heterojunction displayed initial weight loss attributed to the removal of physically attached water molecules and subsequent weight loss due to carbon content combustion (Devi *et al.*, 2020; Irshad *et al.*, 2022). Bismuth ferrite and magnesium-doped bismuth ferrite showed slight weight loss attributed to dehydration and further weight loss related to the breakage of metal-oxygen bonds (Sun *et al.*, 2023). All materials exhibited stability up to 850 °C, indicating their suitability for photocatalytic applications in various temperature conditions.

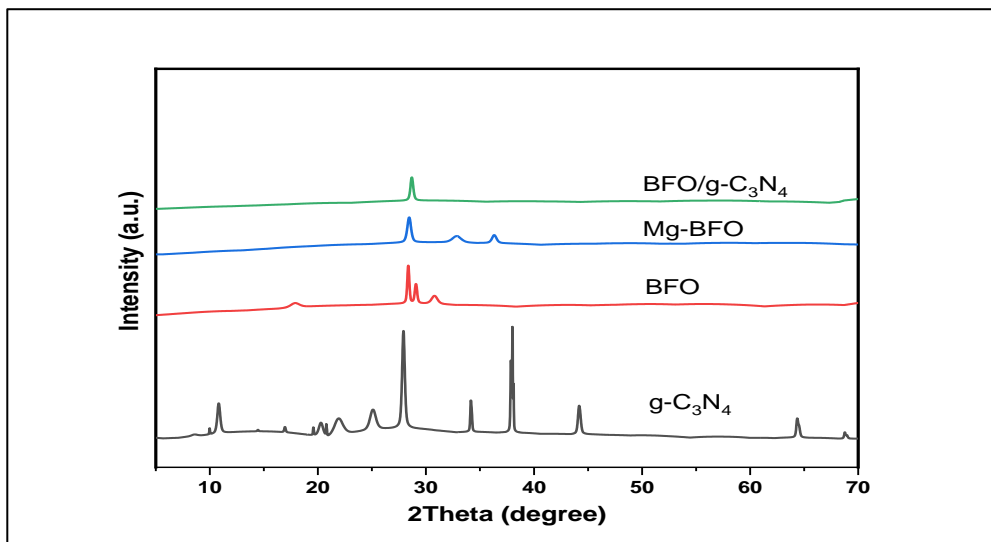


Figure 1: X-ray diffractogram of the synthesized nanostructured materials

Note: $g\text{-C}_3\text{N}_4$ = graphitic carbon nitride; BFO = bismuth ferrite; Mg-BFO = magnesium doped bismuth ferrite; and BFO/ $g\text{-C}_3\text{N}_4$ = heterojunction graphitic carbon nitride/bismuth ferrite

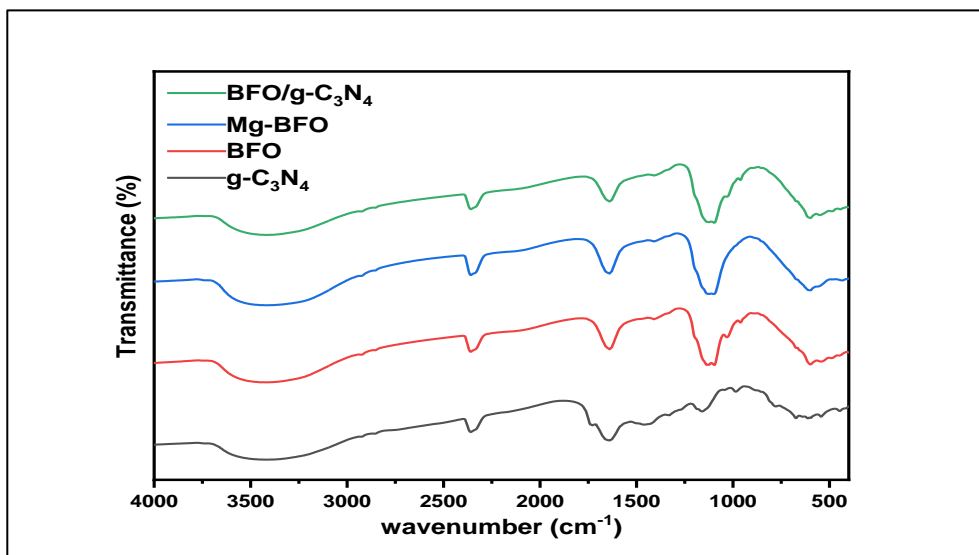


Figure 2: Fourier transform infrared spectra of the synthesized nanostructured materials

Note: $g\text{-C}_3\text{N}_4$ = graphitic carbon nitride; BFO = bismuth ferrite; Mg-BFO = magnesium doped bismuth ferrite; and BFO/ $g\text{-C}_3\text{N}_4$ = heterojunction graphitic carbon nitride/bismuth ferrite

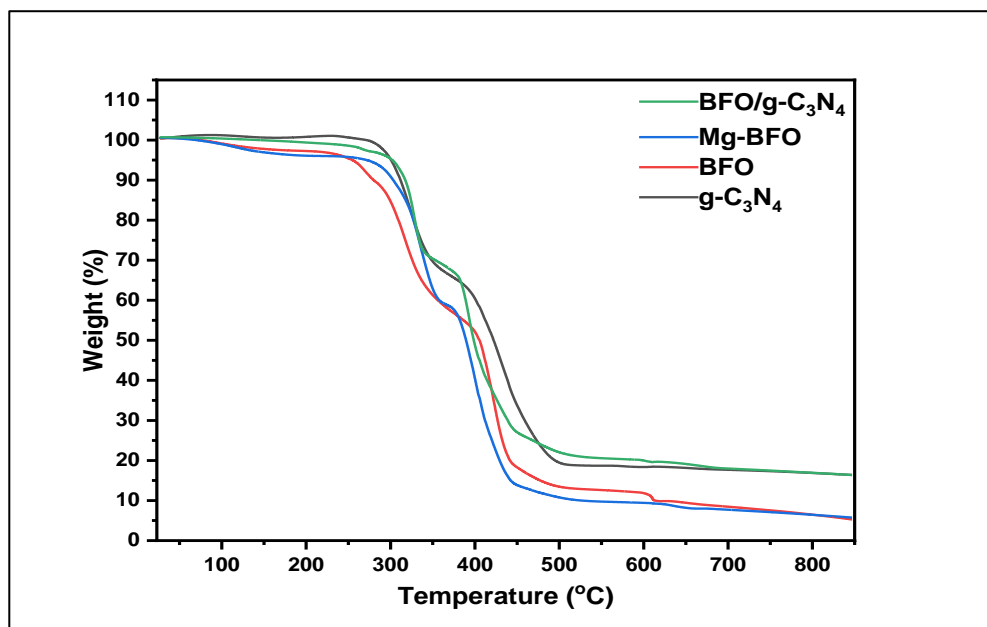


Figure 3: Thermogravimetric analysis profiles of the synthesized nanostructured materials
 Note: g-C₃N₄ = graphitic carbon nitride; BFO = bismuth ferrite; Mg-BFO = magnesium doped bismuth ferrite; and BFO/ g-C₃N₄ = heterojunction graphitic carbon nitride/bismuth ferrite

Effects of Photocatalysts on Maize Growth Performances

Plant height

The effect of synthesized nanostructured materials on plant height is presented in Table 1. The analysis showed that there was a significant ($P < 0.05$) difference between the treatments in all the weeks measured. Across all the weeks, the highest value was recorded in graphitic carbon nitride, while the lowest was recorded in the control treatment. At 2 weeks after sowing (WAS), all the photocatalysts and the +P +K were statistically the same but higher than the recommended rate (RR) and the control. The lower plant height recorded at RR may be as a result of slow-release rate of the fertilizers applied to the crop in the 3 kg pot (Yang *et al.*, 2020) and the nitrogen toxicities to the tender crop (da Silva *et al.*, 2021) at the initial stage. At 3 WAS, RR and graphitic carbon nitride treated soils have statistically the highest and same plant height, followed by the other treatments and the control has the lowest. At 4 and 5 WAS, the trend was similar to that observed in the 4 WAS. At 6 WAS and 7 WAS, RR, bismuth ferrite, graphitic carbon nitride and the +P +K recorded the highest plant height, followed by magnesium doped bismuth ferrite and the heterojunction graphitic carbon nitride/bismuth ferrite, while the control recorded the lowest. It showed that all the catalysts have a positive effect towards the plant height, since none of the catalyst performed less than the control treatment throughout.

For the levels of the treatments (fertilizer and nanomaterials) applied, there was no significant difference between the levels at 2 WAS and 3 WAS. That is, at the initial growing stage, the levels of the catalyst applied performed statistically the same. A significant ($P < 0.05$) difference was observed from 4 WAS up to 8 WAS. Across all the weeks, the highest plant height was recorded in level 2, which is statistically different from level 1 but the same with level 3 at 4 WAS, 6 WAS, 7 WAS and 8 WAS. At 5 WAS, the highest plant height was recorded at level 2, which is statistically higher and different from level 3 and level 1. The result indicated that level 2 (2 g) is the optimum amount of the catalysts to be applied for improve maize performance. This is the same with the RR where level 2 is the actual recommended rate (120:60:60) of the fertilizer, and best maize performance was achieved using the RR (Phares *et al.*, 2022).

Results of the interactions revealed that there are significant ($P < 0.05$) interactions between the fertilizer treatments and the levels of the treatments at 2 WAS, 3 WAS and 5 WAS (Figures 4 – 6). At 2 WAS, the interaction revealed that in all the treatments across levels, only RR has significantly different values where the lowest plant height was recorded in level 1 and is different from level 2 and 3 which are statistically the same. This confirms the result of da Silva *et al.* (2021) that the early-stage toxicities affect the initial growth of maize in the pots. At 3WAS, the highest plant height was recorded in RR at level 1 while the lowest were recorded at level 1, 2 and 3 of the control treatment. Similar trend of plant height at 3 WAS was observed at 5 WAS with only the highest plant height been recorded in graphitic carbon nitride at level 2. Also, the result revealed that all the catalysts have contributed to the development of plant height as they all have values better than the +P +K and the control treatment.

Nanostructured materials in agriculture

Table 1: Effects of synthesized photocatalytic nanostructured materials on maize plant height (cm)

Treatment	Plant height						
	2WAS	3WAS	4WAS	5WAS	6WAS	7WAS	8WAS
Photocatalyst							
Control	28.3d	32.9c	35.9c	40.6c	44.0c	44.9c	45.3c
+ P + K	39.6b	64.7b	82.4b	113.9b	142.3a	156.6ab	161.4ab
RR	34.4c	76.2a	99.4a	121.2a	146.3a	160.3a	168.0a
BiFeO ₃	42.7ab	67.6b	87.9b	114.2b	143.7a	159.8a	166.3a
g-C ₃ N ₄	44.9a	75.8a	99.3a	122.1a	149.2a	163.8a	167.6a
Bi _{0.7} Mg _{0.3} FeO ₃	43.3ab	67.0b	85.7b	109.6b	135.1b	148.2b	150.7b
g-C ₃ N ₄ /BiFeO ₃	39.5b	63.5b	83.9b	109.7b	133.7b	146.8b	152.0b
<i>SE</i> ±	2.17	2.96	3.44	3.36	4.06	4.90	5.44
Level							
1	37.7	61.5	78.5b	100.0b	121.3b	131.9b	137.2b
2	38.9	64.9	85.4a	106.7a	129.0a	142.3ab	146.2a
3	39.8	65.1	82.2ab	102.0b	125.7ab	137.7b	141.6ab
<i>SE</i> ±	1.53	2.09	2.43	2.37	2.87	3.46	3.84
Interaction							
Catalysts*Levels	*	*	NS	*	NS	NS	NS

SE = Standard error; NS = no significant differences; Means with different letters on the same column are significantly different at $P < 0.05$; * = significant at $P < 0.05$; RR = recommended rate; BiFeO₃ = bismuth ferrite; g-C₃N₄ = graphitic carbon nitride; Bi_{0.7}Mg_{0.3}FeO₃ = magnesium doped bismuth ferrite; g-C₃N₄/BiFeO₃ = heterojunction graphitic carbon nitride/bismuth ferrite.

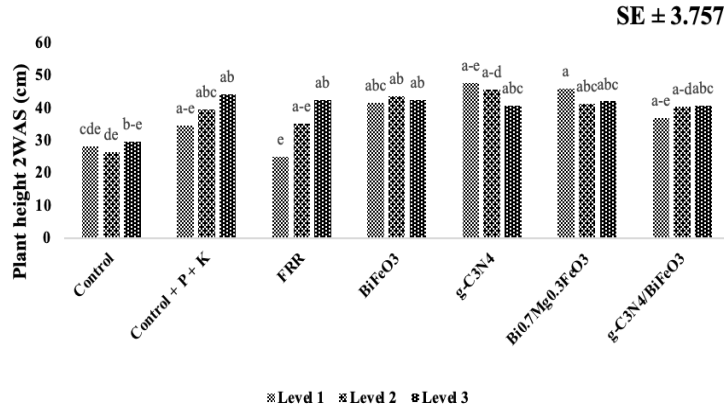


Figure 4: Interaction of fertilizer treatment and level on plant height at 2 weeks after sowing

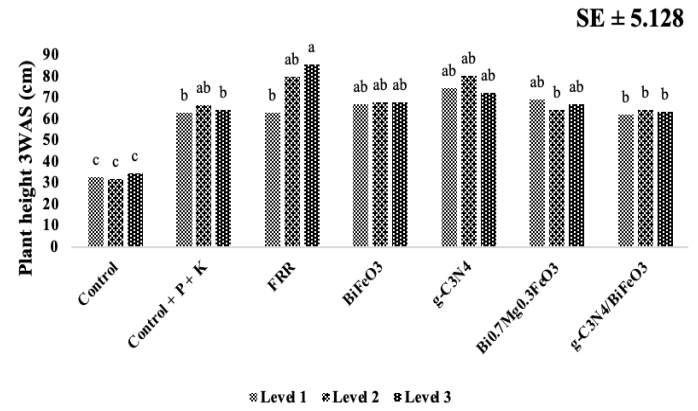


Figure 5: Interaction of fertilizer treatment and level on plant height at 3 weeks after sowing

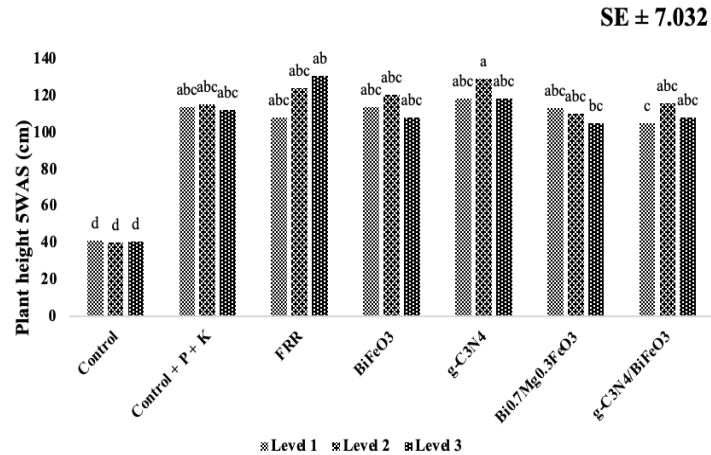


Figure 6: Interaction of fertilizer treatment and level on plant height at 5 weeks after sowing

Stem girth

The effect of synthesized nanostructured materials on stem girth is presented in Table 2. The analysis showed that there was a significant ($P < 0.05$) difference between the treatments at all weeks. Across all the weeks, the highest value was recorded in RR except at 3 WAS, while the lowest was recorded in the control treatment. At 2 WAS, RR was statistically highest of all the treatments. At 3 WAS, RR, bismuth ferrite and heterojunction graphitic carbon nitride/bismuth ferrite were statistically the same. The highest stem girth was recorded in the graphitic carbon nitride while the lowest was recorded in the control. The trend observed in 3 WAS and 4 WAS similar. At 5WAS, 6WAS, 7WAS and 8WAS, RR and magnesium doped bismuth ferrite recorded the highest plant height, followed by bismuth ferrite, graphitic carbon nitride and the heterojunction graphitic carbon nitride/bismuth ferrite, while the control recorded the lowest. Based on the result, it is evident that all the catalysts have a positive effect towards the stem girth, since none of the catalyst performed less than the control treatment.

For the levels of the treatments applied, there was no significant difference between the levels at 4 WAS, 5 WAS and 7 WAS. However significant ($P < 0.05$) differences in stem girth were observed at 2 WAS, 3 WAS, 6 WAS and 8 WAS. Across all the weeks, the highest stem girth was recorded in level 3 of the treatments, which is statistically different from level 1 but the same with levels 2 at 2 WAS and 3 WAS. The highest stem girth under level 3 can be attributed to the higher activities of the catalyst and the higher dose of the NPK fertilizer. This is similar to the result of Singh and Misal (2022) for the NPK fertilizer.

Table 2: Effects of synthesized photocatalytic nanostructured materials on maize stem girth

Treatment	Stem girth (cm)						
	2WAS	3WAS	4WAS	5WAS	6WAS	7WAS	8WAS
Photocatalyst							
Control	0.32d	0.46d	0.44d	0.43b	0.42b	0.42b	0.42c
+ P + K	0.55c	1.11b	1.41bc	1.74ab	1.82a	1.76ab	1.57b
RR	0.69a	1.08c	1.62a	1.73ab	1.91a	1.81ab	1.70a
BiFeO ₃	0.59bc	1.10bc	1.37bc	3.30ab	1.79a	1.67ab	1.59b
g-C ₃ N ₄	0.63b	1.21a	1.48b	1.78ab	1.79a	1.65ab	1.53b
Bi _{0.7} Mg _{0.3} FeO ₃	0.64ab	1.19ab	1.42bc	1.76ab	1.77a	2.77a	1.6ab
g-C ₃ N ₄ /BiFeO ₃	0.56c	1.06c	1.33c	1.78a	1.80a	1.69ab	1.54b
SE ±	0.030	0.062	0.068	0.911	0.099	1.128	0.057
Level							
1	0.54b	0.96b	1.26	1.5	1.54b	1.36	1.33b
2	0.57ab	1.04a	1.28	2.32	1.53b	1.48	1.39b
3	0.60a	1.05a	1.29	1.56	1.66a	1.56	1.47a
SE ±	0.022	0.044	0.048	0.644	0.070	0.798	0.040
Interaction							
Catalysts*Levels	*	*	NS	NS	NS	NS	NS

SE = Standard error; NS = no significant differences; Means with different letters on the same column are significantly different at $P < 0.05$; * = significant at $P < 0.05$; RR = recommended rate; BiFeO₃ = bismuth ferrite; g-C₃N₄ = graphitic carbon nitride; Bi_{0.7}Mg_{0.3}FeO₃ = magnesium doped bismuth ferrite; g-C₃N₄/BiFeO₃ = heterojunction graphitic carbon nitride/bismuth ferrite.

Results of the interactions revealed that there are significant ($P < 0.05$) interactions between the fertilizer treatments and the levels of the treatments at 2 WAS and 3 WAS

(Figures 7 and 8). At 2 WAS, the interaction revealed that in all the treatments across levels, only RR has significantly different values where the highest stem girth was recorded in level 3 and is different from level 2 and 1 which are statistically the same. At 3 WAS, the highest stem girth was recorded across all the treatments and levels with the exception of control where the lowest were recorded at level 1, 2 and 3 of the treatments. This shows that all the catalysts have the same potentials irrespective of the levels applied in terms of the stem girth at the 3 WAS.

Root dry weight

The effect of synthesized nanostructured materials on root dry weight is presented in Table 3. A significant ($P < 0.001$) difference was observed in the treatments. RR ($10.44 \text{ g plant}^{-1}$) recorded the highest root dry weight and is statistically similar to bismuth ferrite ($9.33 \text{ g plant}^{-1}$). Bismuth ferrite, graphitic carbon nitride ($7.89 \text{ g plant}^{-1}$), magnesium doped bismuth ferrite ($7.22 \text{ g plant}^{-1}$), +P +K ($7.67 \text{ g plant}^{-1}$) and heterojunction graphitic carbon nitride/bismuth ferrite ($8.00 \text{ g plant}^{-1}$) were statistically the same but different from the control ($1.04 \text{ g plant}^{-1}$) which recorded the lowest root dry weight. From the result, it is clear that RR has the highest potential of increasing root dry weight followed by bismuth ferrite and the other catalysts, as they all recorded a significantly higher value than the control. However, we cannot conclude that the photocatalytic activities are what resulted to the higher root dry weight, because all the catalysts recorded statistically same root dry weight as the +P +K. Although the catalysts show some promising performances, their contribution to root growth is small compared to the RR. This confirms that the amount of nitrate and ammonium fixed by the photocatalysts is still not up to the plant required nutrient amount (Hao, 2021; Xia *et al.*, 2022).

There was no significant difference observed in the levels of the treatments. The interaction effects were also not significant. The insignificant difference observed in the levels may be as a result of impose volume restriction on the roots in the pot experiment (Ghoto *et al.*, 2020; Muhammad *et al.*, 2022).

Shoot dry weight

The effect of synthesized nanostructured materials on shoot dry weight is presented in Table 3. A significant ($P < 0.001$) difference was observed in the treatments. RR ($75.89 \text{ g plant}^{-1}$) recorded the highest shoot weight. Bismuth ferrite ($62.11 \text{ g plant}^{-1}$), graphitic carbon nitride ($66.67 \text{ g plant}^{-1}$), magnesium doped bismuth ferrite ($58.00 \text{ g plant}^{-1}$), +P +K ($60.21 \text{ g plant}^{-1}$) and heterojunction graphitic carbon nitride/bismuth ferrite ($58.00 \text{ g plant}^{-1}$) were statistically similar but different from the control ($1.08 \text{ g plant}^{-1}$) which recorded the lowest shoot weight. From the result, similar to the root dry weight, it shows that RR has the highest potential of increasing shoot dry weight followed by the other catalysts, as they all recorded a significantly higher value than the control. However, we cannot conclude that the photocatalytic activities are what resulted to the higher shoot dry weight, because all the catalysts recorded statistically same shoot dry weight as the + P + K. Although the catalysts show some promising performances, their contribution to shoot growth is small compared to the RR. This confirms that the amount of nitrate and ammonium fixed by the photocatalysts is still not up to the plant required nutrient amount (Hao, 2021; Xia *et al.*, 2022).

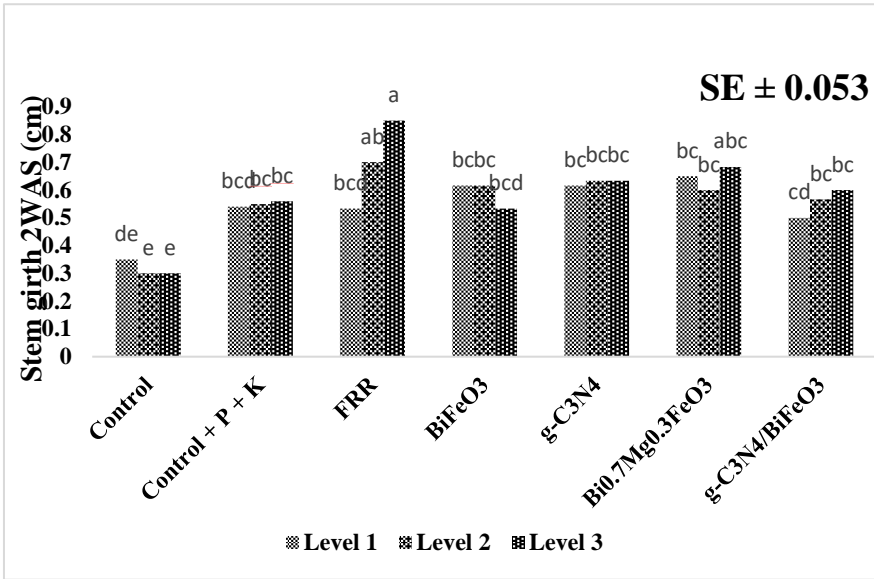


Figure 7: Interaction of fertilizer treatment and level on stem girth at 2 weeks after sowing

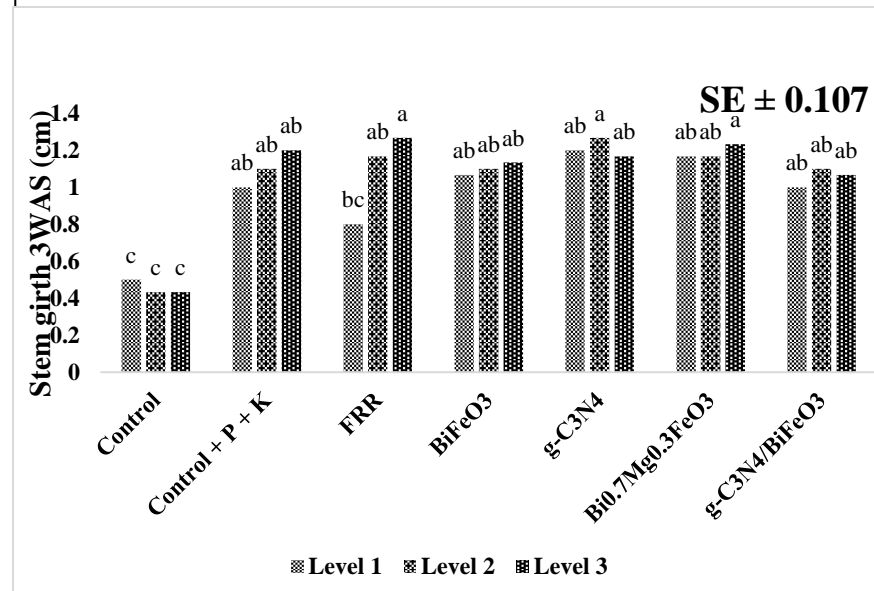


Figure 8: Interaction of fertilizer treatment and level on stem girth at 3 weeks after sowing

Table 3: Effects of synthesized photocatalytic nanostructured materials on maize root dry weight

Treatment	Root dry weight (gplant ⁻¹)	Shoot dry weight (gplant ⁻¹)
Photocatalyst		
Control	1.04c	1.08c
+ P + K	7.67b	60.21b
RR	10.44a	75.89a
BiFeO ₃	9.33ab	62.11b
g-C ₃ N ₄	7.89b	66.67b
Bi _{0.7} Mg _{0.3} FeO ₃	7.22b	58.00b
g-C ₃ N ₄ /BiFeO ₃	8.00b	58.00b
<i>SE</i> ±	1.348	4.645
Level		
1	6.65	45.38c
2	7.17	52.20b
3	8.15	63.29a
<i>SE</i> ±	0.953	3.284
Interaction		
Catalysts*Levels	NS	NS

SE = Standard error; NS = no significant differences; Means with different letters on the same column are significantly different at $P < 0.05$; * = significant at $P < 0.05$; RR = recommended rate; BiFeO₃ = bismuth ferrite; g-C₃N₄ = graphitic carbon nitride; Bi_{0.7}Mg_{0.3}FeO₃ = magnesium doped bismuth ferrite; g-C₃N₄/BiFeO₃ = heterojunction graphitic carbon nitride/bismuth ferrite.

A significant ($P < 0.05$) difference in the shoot dry weights was observed due to the levels of the treatments applied. Level 3 (63.29 g plant⁻¹) recorded the highest shoot weight and is statistically different from level 2 (52.20 g plant⁻¹) and level 1 (45.38 g plant⁻¹) which is the lowest and statistically different from level 2. This shows that the higher the amount of the catalyst applied the higher the shoot dry weight. This result can be directly attributed to the increase in cation exchange capacity (CEC) caused by the higher amount of the catalyst applied. This is because the more you applied the catalyst the more you are increasing the negative surfaces for the cation ion adsorption, and hence the higher the CEC, which translate to the higher soil productivity. No significant interactions effects were observed.

CONCLUSION

The study involved the synthesis and characterization of four distinct photocatalysts (metal-free graphitic carbon nitride, bismuth ferrite, magnesium-doped bismuth ferrite, and a heterojunction of graphitic carbon nitride and bismuth ferrite) with confirmed structural integrity and stability for photocatalytic applications. These catalysts were then applied to assess their impact on the growth performance of maize. Characterization techniques, including PXRD, FTIR, and TGA, validated the suitability of the materials for photocatalytic applications across various temperature conditions. The results revealed significant differences among treatments, with graphitic carbon nitride showing the highest plant height, while the recommended rate (RR) and magnesium-doped bismuth ferrite excelled in stem girth. RR and bismuth ferrite treatments significantly increased root dry weight, emphasizing their positive influence on root development. Similar trends were observed in shoot dry weight, with RR outperforming other treatments. The study highlighted the pivotal role of

treatment levels, identifying level 2 (2 g) as optimal for improved maize performance, aligning with the recommended rate of traditional fertilizer application. While nanostructured materials demonstrated promising performances compared to the control, their impact on growth was comparable to conventional fertilizers. The findings highlight the need for further exploration of the mechanisms underlying nanostructured materials' effects on plant growth, emphasizing the importance of optimizing application levels for maximal benefits in agricultural practices. The study provides a valuable insight into the potential of nanostructured materials for enhancing maize growth, providing a nuanced understanding of their efficacy in comparison to traditional fertilizers.

Acknowledgments

The authors sincerely thank Ahmadu Bello University (ABU), Zaria, Nigeria, and by extension Tertiary Education Trust Fund (TETFUND), Nigeria, for funding this research work under Institution Based Research (IBR) Fund with grant number TETF/DR & D/UNI/ZARIA/IBR/2020/VOL.1/1.

REFERENCES

- Abam, F. I., Nwankwojike, B. N., Ohunakin, O. S., & Ojumu, S. A. (2014). Energy resource structure and on-going sustainable development policy in Nigeria: A review. *International Journal of Energy and Environmental Engineering*, 5(2), 1-16.
- Acharya, R., & Parida, K. (2020). A review on TiO₂/g-C₃N₄ visible-light-responsive photocatalysts for sustainable energy generation and environmental remediation. *Journal of Environmental Chemical Engineering*, 8(4), 103896.
- Akintola, J. (2001). Comparative analysis of the distribution of rainy days in different ecological zones in Nigeria agriculture. *Journal of Environmental Extension*, 2, 31-48.
- Azmy, H. A. M., Razuki, N. A., Aziz, A. W., Satar, N. S. A., & Kaus, N. H. M. (2017). Visible Light Photocatalytic Activity of BiFeO₃ Nanoparticles for Degradation of Methylene Blue. *Journal of Physical Science*, 28(2).
- Babu, S., Singh, R., Yadav, D., Rathore, S. S., Raj, R., Avasthe, R., Yadav, S., Das, A., Yadav, V., & Yadav, B. (2022). Nanofertilizers for agricultural and environmental sustainability. *Chemosphere*, 292, 133451.
- Chen, C. C., & Fan, T. (2017). Study on carbon quantum dots/BiFeO₃ heterostructures and their enhanced photocatalytic activities under visible light irradiation. *Journal of Materials Science: Materials in Electronics*, 28, 10019-10027.
- Devi, K., Sunaja, M., Sandra, R., Revathy, G., Josna, P., & Dephan, U. A. (2020). Synthesis and characterization of CeO₂/Bi₂O₃/gC₃N₄ ternary Z-scheme nanocomposite. *International Journal of Applied Ceramic Technology*, 17(5), 2346-2356.
- Devthade, V., Gupta, A., & Umare, S. S. (2018). Graphitic carbon nitride- γ -gallium oxide (GCN- γ -Ga₂O₃) nanohybrid photocatalyst for dinitrogen fixation and pollutant decomposition. *ACS Applied Nano Materials*, 1(10), 5581-5588.
- Dimkpa, C. O., & Bindraban, P. S. (2017). Nanofertilizers: new products for the industry? *Journal of agricultural and food chemistry*, 66(26), 6462-6473.
- Fox, J. (2018). Using the R Commander in Basic Statistics Courses.

- Ghoto, K., Simon, M., Shen, Z.-J., Gao, G.-F., Li, P.-F., Li, H., & Zheng, H.-L. (2020). Physiological and root exudation response of maize seedlings to TiO₂ and SiO₂ nanoparticles exposure. *BioNanoScience*, *10*, 473-485.
- Hao, Q. (2021). *Novel nanomaterials for efficient photocatalytic ammonia synthesis*
- Harpstead, M. I. (1973). The classification of some Nigerian soils. *Soil Science*, *116*(6), 437-443.
- Haruna, A., Abdulkadir, I., & Idris, S. O. (2020). Synthesis, characterization and photocatalytic properties of Bi_{0.85}-XMXBa_{0.15}FeO₃ (M = Na and K, X = 0, 0.1) perovskite-like nanoparticles using the sol-gel method. *Journal of King Saud University - Science*, *32*(1), 896-903. <https://doi.org/10.1016/j.jksus.2019.05.005>
- Hasija, V., Raizada, P., Sudhaik, A., Sharma, K., Kumar, A., Singh, P., Jonnalagadda, S. B., & Thakur, V. K. (2019). Recent advances in noble metal free doped graphitic carbon nitride based nanohybrids for photocatalysis of organic contaminants in water: a review. *Applied Materials Today*, *15*, 494-524.
- Hu, X., Zhang, W., Yong, Y., Xu, Y., Wang, X., & Yao, X. (2020a). One-step synthesis of iodine-doped g-C₃N₄ with enhanced photocatalytic nitrogen fixation performance. *Applied Surface Science*, *510*, 145413. <https://doi.org/https://doi.org/10.1016/j.apsusc.2020.145413>
- Irshad, A., Warsi, M. F., Agboola, P. O., Dastgeer, G., & Shahid, M. (2022). Sol-gel assisted Ag doped NiAl₂O₄ nanomaterials and their nanocomposites with g-C₃N₄ nanosheets for the removal of organic effluents. *Journal of Alloys and Compounds*, *902*, 163805. <https://doi.org/https://doi.org/10.1016/j.jallcom.2022.163805>
- Jin, B., Yao, G., Jin, F., & Hu, Y. H. (2018). Photocatalytic conversion of CO₂ over C₃N₄-based catalysts. *Catalysis Today*, *316*, 149-154.
- Katsumata, K.-i., Motoyoshi, R., Matsushita, N., & Okada, K. (2013). Preparation of graphitic carbon nitride (g-C₃N₄)/WO₃ composites and enhanced visible-light-driven photodegradation of acetaldehyde gas. *Journal of Hazardous Materials*, *260*, 475-482.
- Luo, H., Yan, J., Shan, Y., Zhou, J., Yu, J., Boury, B., Wu, H., Xiao, H., Huang, L., & Yuan, Z. (2022). Metal-free photocatalyst for nitrogen fixation under visible light based on COF/g-C₃N₄/CNT nanocomposite. *Journal of Environmental Chemical Engineering*, *10*(3), 107713.
- Mardani, R. (2017). The synthesis of Ba²⁺-doped multiferroic BiFeO₃ nanoparticles using co-precipitation method in the presence of various surfactants and the investigation of structural and magnetic features. *Modern Physics Letters B*, *31*(15), 1750169.
- Muhammad, I., Yang, L., Ahmad, S., Mosaad, I. S., Al-Ghamdi, A. A., Abbasi, A. M., & Zhou, X.-B. (2022). Melatonin application alleviates stress-induced photosynthetic inhibition and oxidative damage by regulating antioxidant defense system of maize: A meta-analysis. *Antioxidants*, *11*(3), 512.
- Singh, S., & Misal, N. (2022). Effect of different levels of organic and inorganic fertilizers on maize (*Zea mays* L.). *Indian Journal of Agricultural Research*, *56*(5), 562-566.
- Souza, A. M. G. P., Silva, G. R. O., Santos, J. C. d., Martinelli, D. M., Souza, M. J. B. d., & Melo, D. M. A. (2010). Synthesis and characterization of LaNi_xCo_{1-x}O₃ perovskites via complex precursor methods.
- Sun, Z., Wei, J., Li, Y., Liu, Z., Xiahou, M., Chen, G., Zhao, L., & Cheng, Z. (2023). Coupling oxygen vacancy gradient distribution and flexoelectric effects for enhanced

- photovoltaic performance in bismuth ferrite films. *Inorganic Chemistry Frontiers*, 10(4), 1315-1327.
- Team, R. C. (2017). *R: A language and environment for statistical computing*. Vienna, Austria: R Foundation for Statistical Computing; 2017. ISBN3-900051-07-0 <https://www.R-project.org>.
- Thomas, A., Fischer, A., Goettmann, F., Antonietti, M., Müller, J.-O., Schlögl, R., & Carlsson, J. M. (2008). Graphitic carbon nitride materials: variation of structure and morphology and their use as metal-free catalysts. *Journal of Materials Chemistry*, 18(41), 4893-4908.
- Wojtyła, S., & Baran, T. (2021). Multi-technical study of copper oxide on graphitic carbon nitride and its role in the photocatalytic reactions. *Nano Select*, 2(2), 389-397. <https://doi.org/https://doi.org/10.1002/nano.202000221>
- Xia, P., Pan, X., Jiang, S., Yu, J., He, B., Ismail, P. M., Bai, W., Yang, J., Yang, L., & Zhang, H. (2022). Designing a redox heterojunction for photocatalytic “overall nitrogen fixation” under mild conditions. *Advanced Materials*, 34(28), 2200563.
- Zhang, G., Sewell, C. D., Zhang, P., Mi, H., & Lin, Z. (2020). Nanostructured photocatalysts for nitrogen fixation. *Nano Energy*, 71, 104645.